A PILOTED COMPARISON OF ELASTIC AND RIGID BLADE-ELEMENT ROTOR MODELS USING PARALLEL PROCESSING TECHNOLOGY

Gary Hill
NASA Ames Research Center
Mountain View, CA

and

Ronald W. Du Val, John A. Green and Loc C. Huynh
Advanced Rotorcraft Technology, Inc.
Mountain View, CA

Abstract

A piloted comparison of rigid and aeroelastic blade-element rotor models was conducted at the Crew Station Research and Development Facility (CSRDF) at Ames Research Center. FLIGHTLAB, a new simulation development and analysis tool, was used to implement these models in real time using parallel processing technology. Pilot comments and quantitative analysis performed both on-line and off-line confirmed that elastic degrees of freedom significantly affect perceived handling qualities. Trim comparisons show improved correlation with flight test data when elastic modes are modeled. The results demonstrate the efficiency with which the mathematical modeling sophistication of existing simulation facilities can be upgraded using parallel processing, and the importance of these upgrades to simulation fidelity.

Introduction

Developing the next generation of advanced rotorcraft—capable of higher speeds and greater maneuverability, with precise, superaugmented control systems and hingeless rotors—will require expanded-bandwidth, real-time simulations that include aeroelastics and structural dynamics. These disciplines can no longer be left uncoupled, and more engineers on the design staffs will need access to these higher fidelity simulations. Advanced Rotorcraft Technology (ART), Inc., the U.S. Army Aeroflightdynamics Directorate, and NASA Ames's Military Technology Office have pursued parallel processing as a cost-effective means of meeting this need. In a series of research activities, rotorcraft models of increasing complexity have been parallelized for real-time operation. Under a Small Business Innovative Research Program (SBIR), a piloted workstation was developed, which was driven by a MicroVAX II computer converted to a parallel processor by adding four processor boards to the MicroVAX's backplane. On that parallel processor, the Rotor Systems Research Aircraft/X-Wing (RSRA/X-Wing), with possibly the most complex aerodynamic interactions ever modeled, was flown through conversions between rotary and fixed wing (Ref. 1). Later, the same modified MicroVAX II replaced the aerodynamic rotor map with a blade-element representation on a UH-60 Black Hawk training simulator at Fort Ord, California, and piloted comparisons were performed (Ref. 2). This paper reports on an extension of this technology to a blade-element rotor model that adds aeroelastics and structural dynamics. Again with the UH-60 as the subject, this "global" simulation model with blade flexibility was demonstrated in real time on two commercial parallel processor computers, and interfaced with the Army's Crew Station Research and Development Facility (CSRDF) at the NASA Ames Research Center.

Objectives

As a follow-on to the effort at Fort Ord (Ref. 2), this study had four objectives. The first was to develop a free-flight rotorcraft simulation model with aeroelastic and structural dynamics modeling; the second was to design a parallel processing architecture for this global model to permit real-time operation; the third was to run the real-time simulation interactively with a full-simulation facility; and the fourth was to perform piloted simulations comparing the model with conventional rigid body modeling.

Methods

In this study, the global simulation was developed and adapted for parallel processing using ART, Inc.'s FLIGHTLAB system, a tool for developing optimal parallel software architectures for real-time operation from a modular library of elements. FLIGHTLAB includes

1. A library of simulation elements to synthesize a desired vehicle configuration, a dynamic assembler, and a solver routine.

2. An interactive programmer's workstation for developing and optimizing parallel architectures by decomposition, mapping, and profiling.

3. An engineer's workstation for on-line, real-time data access and engineering analysis. This workstation is also interactive, with symbolic data access, high-level engineering analysis, and graphical display capabilities.

4. A pilot's workstation with a three-axis side arm controller and an out-the-window visual scene with a head-up display (HUD).

Blade-element aerodynamic rotor models divide each rotor blade into segments and use airfoil tables to compute each segment's aerodynamic load from the angle of attack, Mach number, and dynamic pressure produced by local motion and flow. Air loads from the segments are summed to derive forces about the blade degrees of freedom and to calculate reactions at the hub. Both the rigid and the elastic blade modeling include hub motion, flapping and lead-lag hinge articulation, and blade feathering.

The global model is a free-flight, aeroelastic, blade-element model. Blade aeroelastics and structural dynamics are modeled by mode shapes derived from finite-element analysis. When the modal representation is added to the rigid blade-element model, the number of blade elements has to be doubled from five segments per blade to ten in order to attain fidelity of the high-frequency dynamics. The global model contains hinge articulations in addition to coupled elastic degrees of freedom.

FLIGHTLAB's free-flight rigid-blade-element model was validated by matching the UH-60 blade element model of the NASA version of Sikorsky Aircraft's Master General Helicopter Program (GENHEL) (Ref. 3). This simulation model of the UH-60 helicopter, obtained from Sikorsky, has been updated at NASA Ames and validated against flight test data (Ref. 4). The FLIGHTLAB aeroelastic rotor model was validated against Lockheed's REXOR aeroelastic rotor model (Ref. 5), and the global (free-flight aeroelastic) model was validated against available flight test data (Ref. 6). FLIGHTLAB's unique data-driven configuring capability facilitated the comparative analysis and validation. Modifications such as the interchange of elastic and rigid modules and altering the hinge sequence in the modeling would require extensive recoding in most simulation models.

After creating and validating the global model, parallel architectures were designed to provide a real-time capability. Using FLIGHTLAB's parallelizing features, it was determined that an eight-node (each node is an individual CPU) parallel computer, each node having a CPU speed approximately 17 times faster than the MicroVAX II, would suffice. The global model was then benchmarked in serial mode on commercial parallel processors of the class RISC. Speeds of up to 21 times that of the MicroVAX II were obtained; thus it appeared that real time was feasible.

The next step, that of actually running the massive global model in real time, was facilitated by the cooperation of the computer manufacturers, who provided technical assistance and generous nonreimbursed access to their computers. The two parallel-processing computer systems used were a Silicon Graphics IRIS (SGI) 4D/280 GTX with eight processors, and a BBN TC2000 with sixteen processors. Identical parallel architectures were installed on both, and real time was confirmed by timing checks and simulated flight from the pilot workstation. Interface to the CSRDF's VAX 8650 host computer was through Ethernet. Existing visual and cockpit protocols remained intact while the vehicle's simulation math model, on the host computer, was replaced by the math model running under FLIGHTLAB on the parallel platforms.

The complete Blackhawk simulation model was updated every 10 deg of rotor azimuth travel, which resulted in a 6-msec integration cycle. The parallel processing architecture is shown in Fig. 1. This architecture was implemented on the eight-processor SGI computer and eight of the sixteen BBN computer processors. It used five processors for the math model: four procressors dedicated to the rotor (one per blade), and one processor for the fuselage, tail, control system, and engine model. A sixth processor drove an engineer's workstation, and a seventh served the Ethernet interface to the CSRDF host VAX 8650 at 60 Hz. Integration of the parallel processor with the CSRDF is shown schematically in Fig. 2.

Pilot tasks were chosen to assess the effects of aeroelastic degrees of freedom on perceived fidelity. Hover maneuvers included bob up/bob down and lateral dash/quick stops. High-speed flight maneuvers included slalom maneuvers that require rapid bank reversals to control lateral position, and dolphin maneuvers with rapid collective changes to control vertical position. The pilots performed frequency sweeps to collect engineering data.

Results and Discussion

The following analysis compares trim, stability, and dynamic responses of the rigid and aeroelastic blade-element models. There are differences between the two simulation models in all three areas, especially at high speed.

Longitudinal trim of the rigid and elastic models are compared with flight test data (Ref. 6) in Fig. 3. Pitch attitude, longitudinal cyclic position, and collective position are plotted for flight speeds from –50 to 160 knots. At low speeds, the rigid and elastic models show little difference in their trim characteristics. At hover, pitch attitude and longitudinal cyclic position agree well, but results for both rigid and elastic models deviate from flight test results at transition speeds. This deviation could be caused by the extreme sensitivity to horizontal stabilator incidence setting, which the flight control system programs as a function of airspeed in the transition range. Stabilator position is not specified for the flight test data, and may differ from that of the production aircraft. However, the trim parameters do show proper trends, which is most important for handling-qualities analysis. Trim comparisons for

lateral/directional axes are not included, as differences were inconclusive or less significant.

The rigid and elastic model differences are greater at higher airspeeds. The amplitude of the rotor differential equation's periodic coefficients increases with advance ratio, causing greater interharmonic coupling. This airspeed-dependent effect is present in both the rigid and the elastic models, but is exaggerated in the elastic model due to the added high-frequency content. The widest differences occur at 160 knots, and are seen in pitch attitude (4 deg) and collective position (2 in.), on the right side of Fig. 3. Significantly more collective control is required to produce the same thrust, because flexed blades generate less out-of-plane lift than unflexed blades do, and thrust is the integral of lift component over the rotor. The increased in-plane component of lift due to blade flexibility and the additional airfoil drag due to higher collective pitch combine to significantly increase the effective rotor drag, requiring more pitch-down attitude to balance the drag with the thrust.

The accuracy of both the NASA Ames and Sikorsky Aircraft UH-60 GENHEL simulation models has been improved by the use of a quasi-static approximation to blade flexibility derived from flight test data. In Fig. 4, this "dynamic twist" approximation is added to the FLIGHTLAB rigid blade model and significantly improves the fit at high speed. The aeroelastic model, however, still provides a closer fit to the flight test data, and does not require tuning since its improved fit results from higher fidelity physical modeling. We shall see that the global model also represents transient elastic effects.

To compare stability characteristics of the rigid and elastic models, a six-degree-of-freedom linear model with eight state variables was constructed by making perturbations about the trim points. Roots of the linearized models were collected a sufficient time after the perturbations to allow higher frequency modes to reach steady-state, assuring an accurate quasi-static approximation for these modes.

Damping ratio and natural frequency of the roll/pitch, short period, and dutch roll modes are plotted against airspeed for the rigid and elastic models in Fig. 5. High-frequency elastic modes would normally not be expected to affect the six-degree-of-freedom response significantly, but these results show that there is an impact from elasticity on the stability characteristics. The greatest differences occur at higher airspeed, as is the case with trim. Since linearized models represent the open-loop dynamics, this effect is not related to control-system coupling, and the airspeed dependence suggests that the periodic coefficient effect is again responsible for the coupling of elastic effects into the handling-qualities range.

Examining the roll/pitch mode damping and natural frequency in Fig. 5(a), we find that the roots are decoupled and aperiodic, but at high speed they coalesce into a coupled periodic roll/pitch mode. The frequency of this coupled mode is quite different at high speed for the elastic and rigid models. The damping, however, is relatively similar for the two cases. The short-period mode (Fig. 5(b)) is unstable for most of the speed range for both models, although the elastic model has more stability than the rigid model does at high speed. The dutch-roll mode (Fig. 5(c)) is stable for most of the speed range in both models although a significant reduction in damping for the elastic model is seen at speeds greater than 100 knots, resulting in instability at 140 knots, whereas the rigid model remains reasonably stable. The heave mode and the spiral mode do not exhibit much difference between rigid and elastic models, and are not shown.

Next we compare dynamic responses of the rigid and elastic models. Figures 6 and 7 show the pitch rate response to 3-2-1-1 longitudinal cyclic input for both open loop control and with the stability augmentation system (SAS) on. Figure 6 shows data for the models at hover, where, in the open loop response, a small trim difference increases with time, because of the unstable short period pitch mode identified in Fig. 5. But with the SAS on, providing a low-gain feedback, no difference between elastic and rigid models is observed, because the low-gain SAS stabilizes the models without creating additional coupling of the elastic response into the handling-qualities range.

The open-loop and SAS-on time responses are again compared in Fig. 7, but this time at 150 knots forward speed. The rigid model exhibits a significantly different open-loop time response than the elastic model does, confirming the trend of the stability analysis in Fig. 5. Pitch response of the rigid model is seen to be more divergent, as predicted in the linear analysis in Fig. 5 for the short-period pitch mode. The reduced response of the elastic model to the 3-sec and 2-sec steps indicate a reduction in stick sensitivity for low frequency inputs; and the increased response of the elastic model to the higher frequency 1-sec doublet in the 3-2-1-1 input demonstrates significant elastic excitation and coupling with the airframe degrees of freedom. With the SAS on, the pitch rate drops off to almost nothing at the end of the first pulse for the elastic model, but the response to high-frequency inputs is virtually identical for both cases. The SAS appears to be suppressing the differences observed in the open-loop rotor models for the higher frequency inputs, but low-frequency differences, such as those due to the different trim conditions, are still significant. It is obvious that the higher order dynamics do affect handling qualities, and need to be considered in the formulation of flight control laws at higher speeds. These plots were generated off-line, but their accuracy was later confirmed during the piloted simulations.

To further demonstrate the impact of elasticity on closed loop control as a function of flight condition, frequency responses were obtained for the hover and 150-knot cases with the SAS on. Figure 8 shows the pitch-rate response to longitudinal cyclic control for both rigid and elastic models. The magnitude of the transfer function is presented in the upper plots and the phase is given in the lower plots, in both as a function of frequency of the input. The comparison again shows virtually no difference for the hover case. At 150 knots the two models are seen to differ significantly at low frequency, but they exhibit no noticeable differences at high frequency. This is consistent with the time-domain results of Fig. 7 and further indicates that the SAS suppresses the rotor modeling differences in the higher frequency range.

From the analytic phase, the study proceeded to the piloted simulation phase. Installation and interface of the parallel processing computers at the CSRDF was accomplished in only three weeks and was followed by two weeks of piloted evaluation. Both NASA and Army test pilots participated in the evaluation, some of whom were involved in the rotor-map versus blade-element comparison at Fort Ord (Ref. 2). Data collected on-line using the engineers workstation was correlated with pilot comments, off-line comparisons, and flight tests.

The CSRDF simulator cockpit is equipped with dual, four-axis side-stick controllers in lieu of conventional cyclic and collective. The UH-60 SAS and the flight-path stabilization (FPS) control system were modified to use the CSRDF side arm controllers in place of the center stick and collective lever. The opportunity was taken to also integrate the advanced control system known as ADOCS, the advance digital optical control system, from the facility (Ref. 7). Since the original UH-60 control laws were not intended for a side stick arrangement, is it not surprising that the ADOCS control system was preferred.

In Fig. 9, the elastic and rigid models are compared for low-gain SAS and advanced high-gain ADOCS. Amplitude of and phase of the pitch-rate frequency response to longitudinal cyclic control, at hover, is shown for SAS on at the left in Fig. 9 just as it was in Fig. 8, and no differences between rigid and elastic models are noted. With the ADOCS controller, as shown on the right in Fig. 9, the static gain is five times greater than that of the SAS and a significant difference is exhibited between the rigid and elastic models, particularly in the higher frequency range. The elastic model is seen to be considerably less sensitive to pilot inputs than the rigid model is, an effect that was consistently observed by the pilots. Since there are no periodic coefficient effects at hover, these differences are attributed to coupling between elastic and rigid body modes induced by the high-gain ADOCS controller. Since high-gain controllers are the way of the future, the importance of the elastic modeling, even at hover, is demonstrated.

More comparisons between rigid and elastic models with the ADOCS configuration are shown in Figs. 10 through 12. The formats are taken from the recently issued ADS-33C handling qualities specification (Ref. 8). The equivalent time delay versus bandwidth for the elastic and rigid models is plotted in Fig. 10. The frequency response data for the pitch attitude response to longitudinal cyclic control at 80 knots is shown at the bottom of the figure. The bandwidth and equivalent time delay shown in the top graph were taken from these plots. Elastic and rigid models are both to the right of the level-1/level-2 border, but blade elastics half the level-1 margin.

Figure 11 shows the vertical response to collective input with the ADOCS controller at hover. Time response of the rigid and elastic models to a collective step is shown at the bottom of the figure with the curve fit of the low-order equivalent altitude response model overlaid. The curve fit is good in both cases. The identified time constant and time delay parameters of the low-order equivalent response models are shown in the tables at the top of the figure for the rigid and elastic models and compared with the ADS-33C specification for level-1 and level-2 response. Responses were similar for both elastic and rigid models, and are well within the level-1 category for both cases.

Figure 12 shows an "attitude quickness" comparison of rigid and elastic models at 80 knots using the ADOCS. The time response plots at the bottom of the figure show the longitudinal cyclic input and the resulting pitch-rate and pitch-attitude responses for specific elastic and rigid trials. The increased level of control input required to achieve the same pitch response with the elastic model is a result of the reduced sensitivity of the elastic model. This effect was previously noted, in the time-response plots of Fig. 7 and the frequency-response plots of Figs. 8 and 9. This characteristic was repeatedly confirmed by the pilots, and they felt that the elastic model response was more realistic. The top plot, of the peak pitch rate to peak attitude change ratio versus peak attitude change, is representative of maneuverability or quickness; it shows a significant difference between rigid and elastic models for the 80-knot flight condition, although both models are well within the level-1 boundary.

Conclusions

The following conclusions were drawn from this investigation.

1. The ability to process the aeroelastic model in real time on both the SGI and BBN parallel-processing systems was successfully demonstrated.

2. The ability of parallel processors to support a real-time interface with a full-simulation facility while maintaining real-time operation was demonstrated.

3. The aeroelastic free-flight model compared well with flight test data in off-line comparisons, and exhibited improvements both statically and dynamically over the rigid blade model.

4. Pilots perceived the effect of the aeroelastic degrees of freedom on the handling qualities and rated this effect as an enhancement of simulation fidelity.

The comparisons between the rigid and aeroelastic models demonstrated two mechanisms for coupling between the high-frequency elastic modes and the low-frequency airframe response. A speed-dependent effect, probably due to interharmonic coupling produced by the periodic-coefficient rotor model, resulted in significant differences between rigid and elastic trim conditions at high speed; comparison with flight test data confirmed the elastic model to be more accurate. A gain-dependent effect was demonstrated by comparison of SAS and ADOCS responses at hover. The high-gain ADOCS was seen to produce significant coupling of the elastic degrees of freedom with the airframe response, whereas the low-gain SAS suppressed dynamic differences in the rotor models without producing additional coupling. A comparison of open-loop stability characteristics versus airspeed showed a speed-dependent difference that tended to stabilize the short-period mode and destabilize the dutch-roll mode. A comparison of rigid and elastic models using the ADS-33C handling qualities criteria further demonstrated a significant difference between the two models and quantitatively supported the pilot's qualitative assessment that the elastic model was significantly less sensitive to control inputs than the rigid model was.

The primary impact of using parallel-processing technology in rotorcraft simulation is expected to be greater productivity. The most immediate impact will be elimination of the recoding and verification usually required when the simulation model is taken to a large simulation facility. The ability of smaller, less expensive computers to drive larger facilities means there will be backup computers to allow more continuous operation of the expensive visual and motion bases, and additional machines for preparing the next entry. The common on-line engineering-and-analysis tool will also realize substantial savings.

A second advantage is that the inclusion of aeroelastics and structural dynamics in the simulation model will increase the fidelity of rotorcraft real-time simulations. Inclusion of these disciplines are a necessity for the development of high-speed and high-agility rotorcraft. Hingeless rotors, high-gain flight control systems, higher harmonic control (active vibration suppression), all require concurrent engineering.

A third advantage is achieved by lowering the cost of computers capable of running blade-element models. These more physical representations add fidelity to training simulators, tie the trainer simulation model to the engineering simulation model, reduce expensive tuning, and provide greater flexibility to modify the model for aerodynamic changes.

The FLIGHTLAB system provides a unified tool for the development, parallelization, analysis, and real-time operation of flight simulations. Its use in this application expedited the cost-effective utilization of the CSRDF facility.

Acknowledgments

The authors would like to thank the Army Aeroflightdynamics Directorate at Ames Research Center and, in particular, the Crew Station Research and Development Branch for providing both access to the CSRDF and the necessary support personnel to carry out this investigation. They would also like to thank Alex Gallico and Guy Beauchesne of CAE Electronics for their help and support.

References

1. Du Val, R. W., "A Real-time Blade Element Helicopter Simulation for Handling Qualities Analysis," Proceedings of the Fifteenth European Rotorcraft Forum, Amsterdam, Sept. 1989.

2. Corliss, L., and Du Val, R. W., "A Comparison of Blade-Element and Rotor-Map Helicopter Simulations Using Parallel Processing," Proceedings of the 46th Annual Forum of the American Helicopter Society, Washington, D.C., May 1990.

3. Ballin, Mark G., "Validation of a Real-Time Engineering Simulation of the UH-60A Helicopter," NASA TM-88360, Feb. 1987.

4. Ballin, Mark G., "Validation of the Dynamic Response of a Blade Element UH-60 Simulation Model in Hovering Flight," Proceedings of the 46th Annual Forum of the American Helicopter Society, Washington, D.C., May 1990.

5. Reaser, J.S., and Kretsinger, P.H., REXOR II Rotorcraft Simulation Model-Volume I—Engineering Documentation, Lockheed-California Co., NASA CR 145331, June 1978.

6. Singer Link Trainer Test Procedures and Results Report (TTPRR) for the UH-60 Black Hawk Trainer, Singer Link, Mar. 1989.

7. Advanced Digital/Optical Control System (ADOCS) Flight Demonstrator Program, Interim Technical Report—Detailed Design, Boeing Vertol Company Report No. D358-10045-1, May 1983.

8. Aeronautical Design Standard, Handling Qualities Requirements for Military Aircraft, United States Army Aviation Systems Command, St. Louis, MO, Directorate for Engineering, ADS-33C, Aug. 1989.

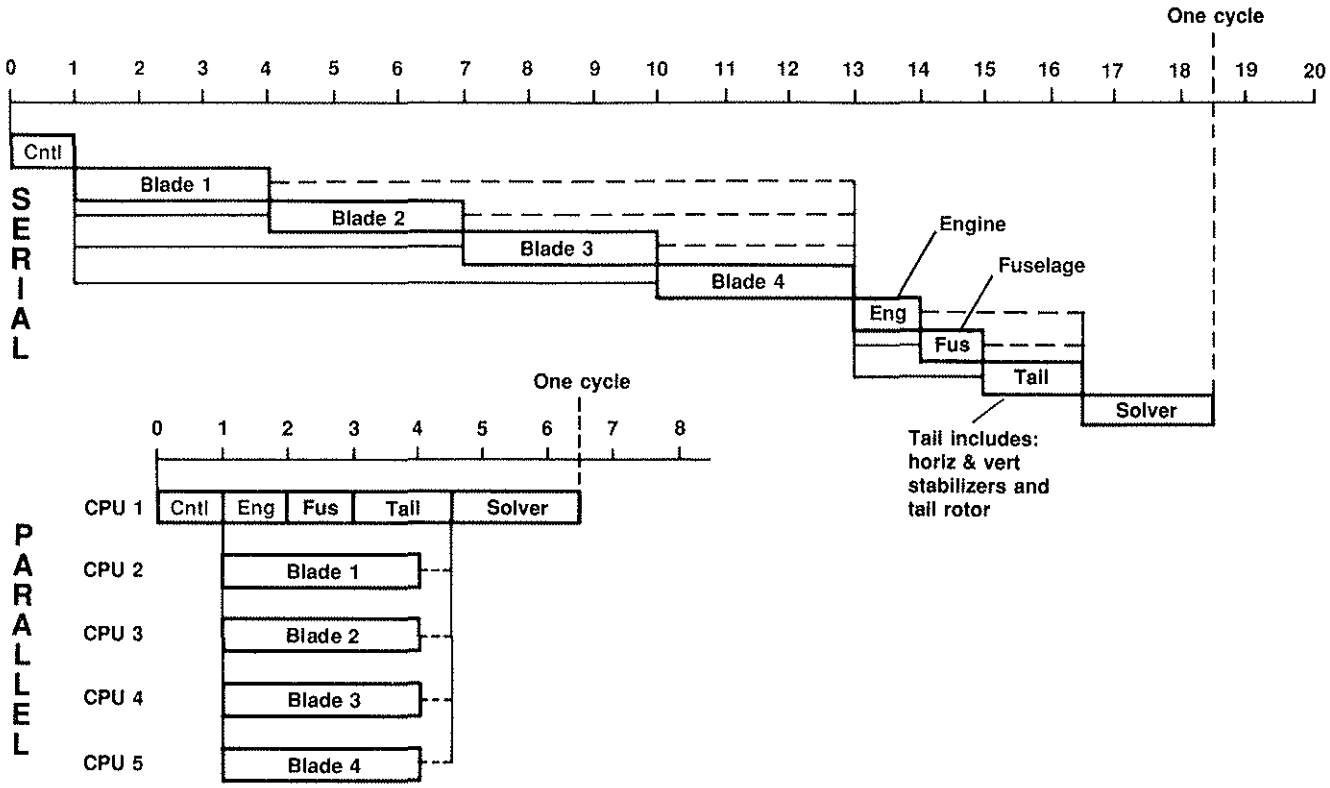

Figure 1. The parallelization process.

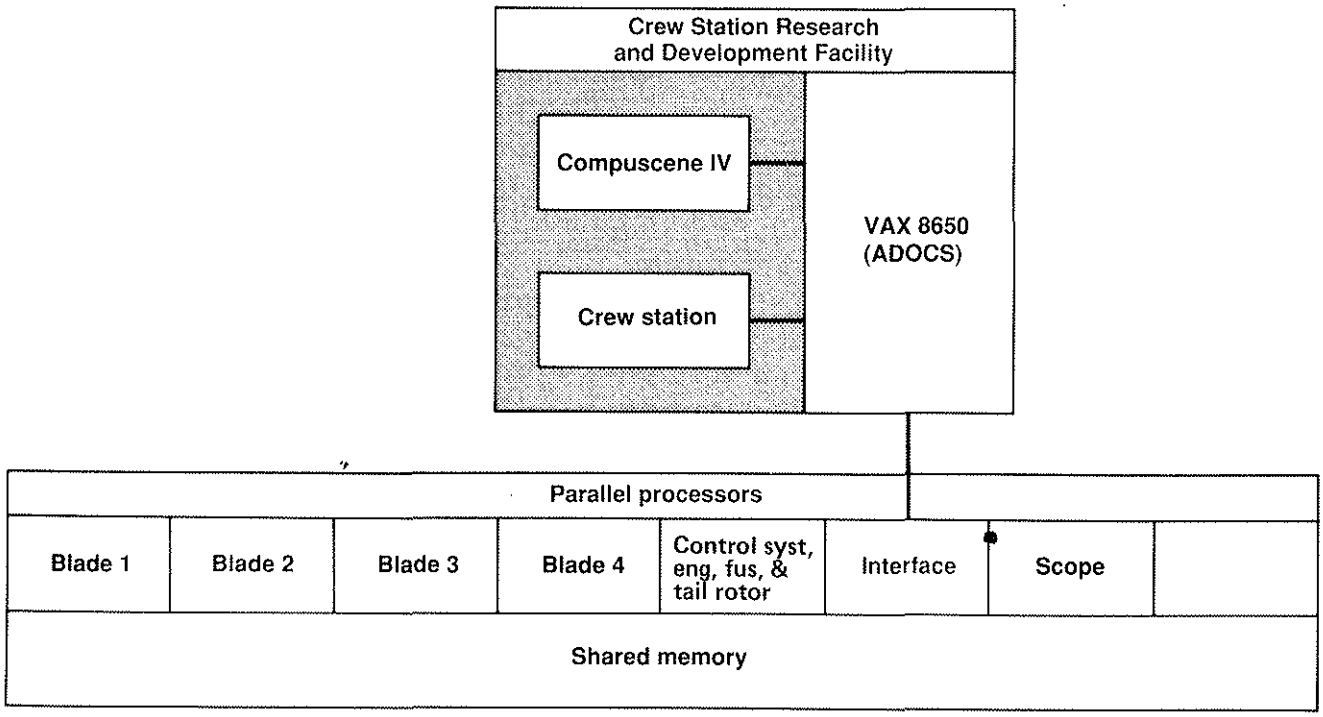

Figure 2. CSRDF/parallel processor architecture.

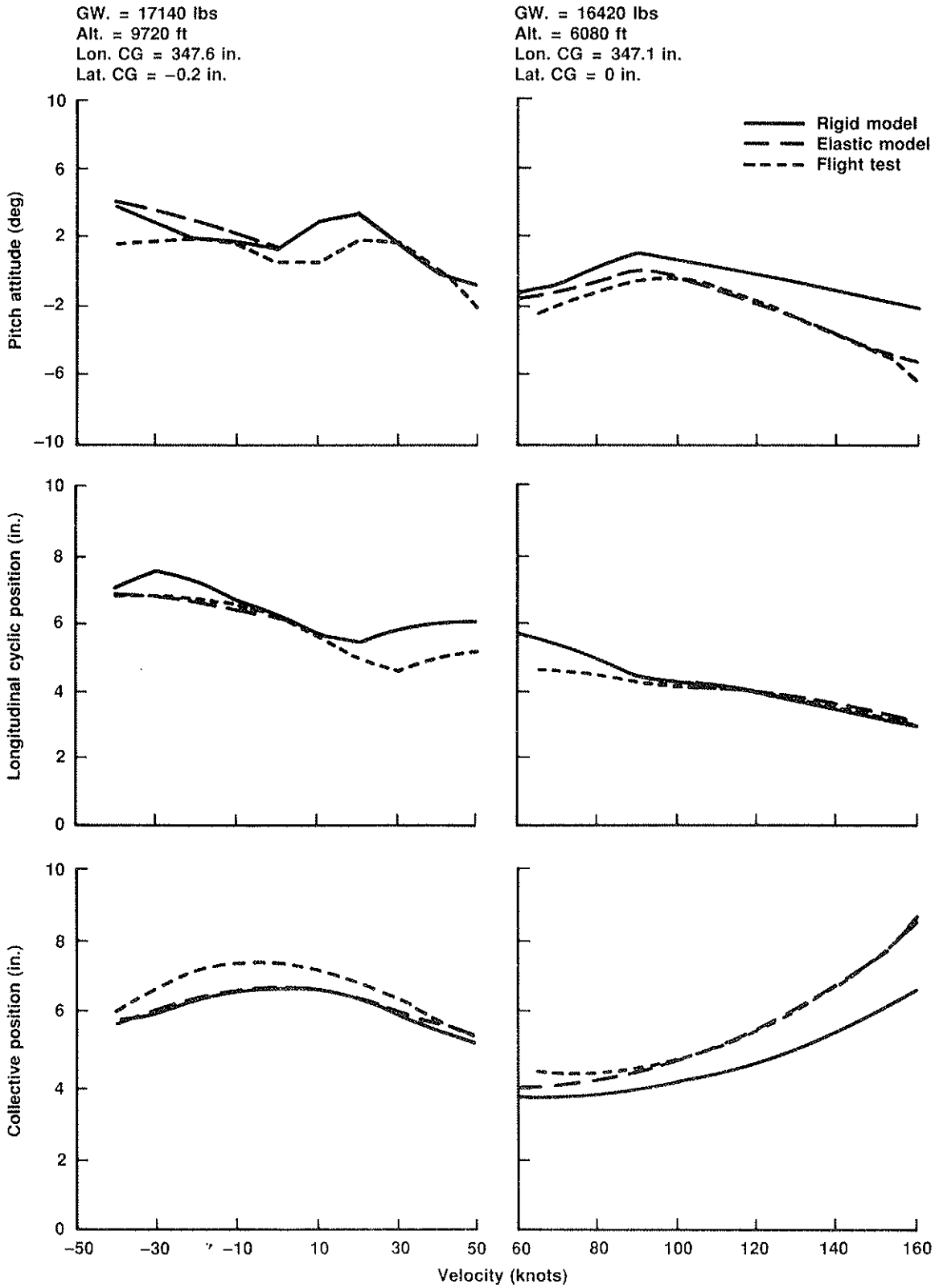

Figure 3. Trim comparison of rigid and elastic models with flight test data.

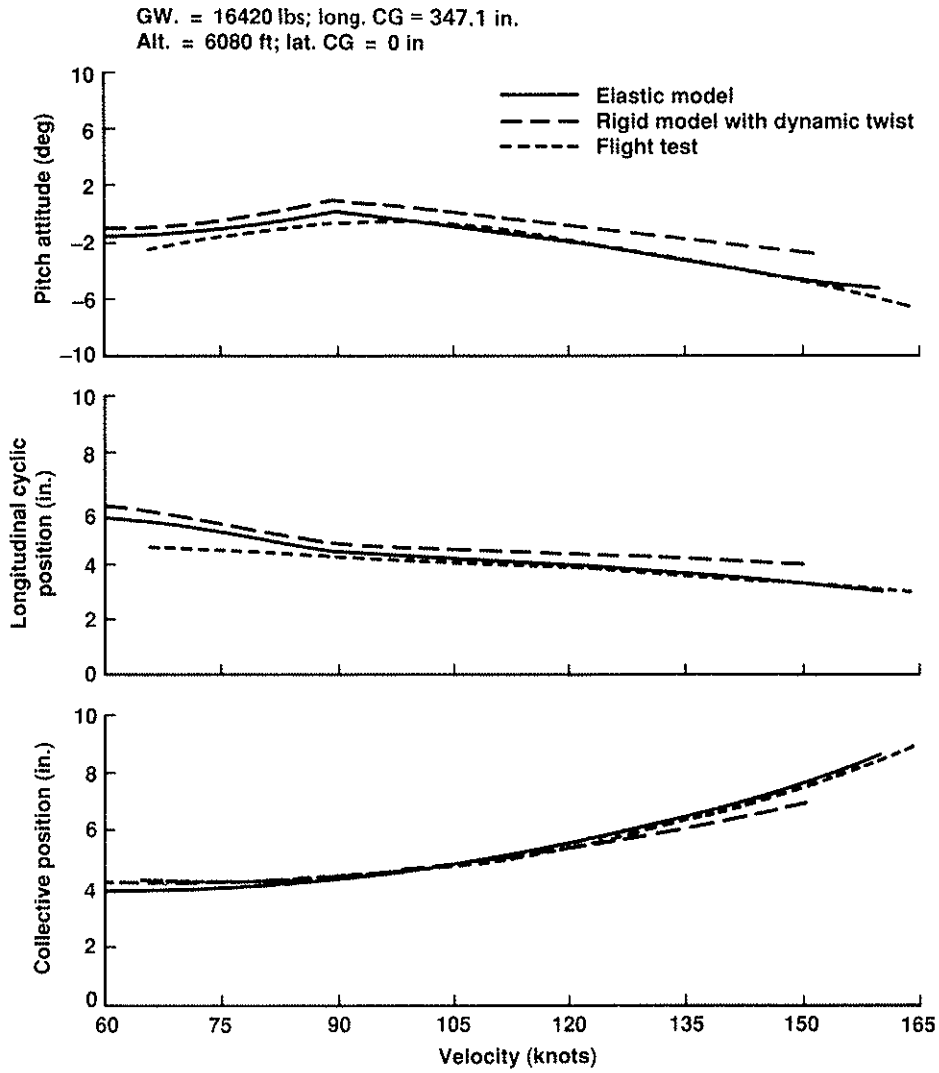

Figure 4. Trim comparison using dynamic twist.

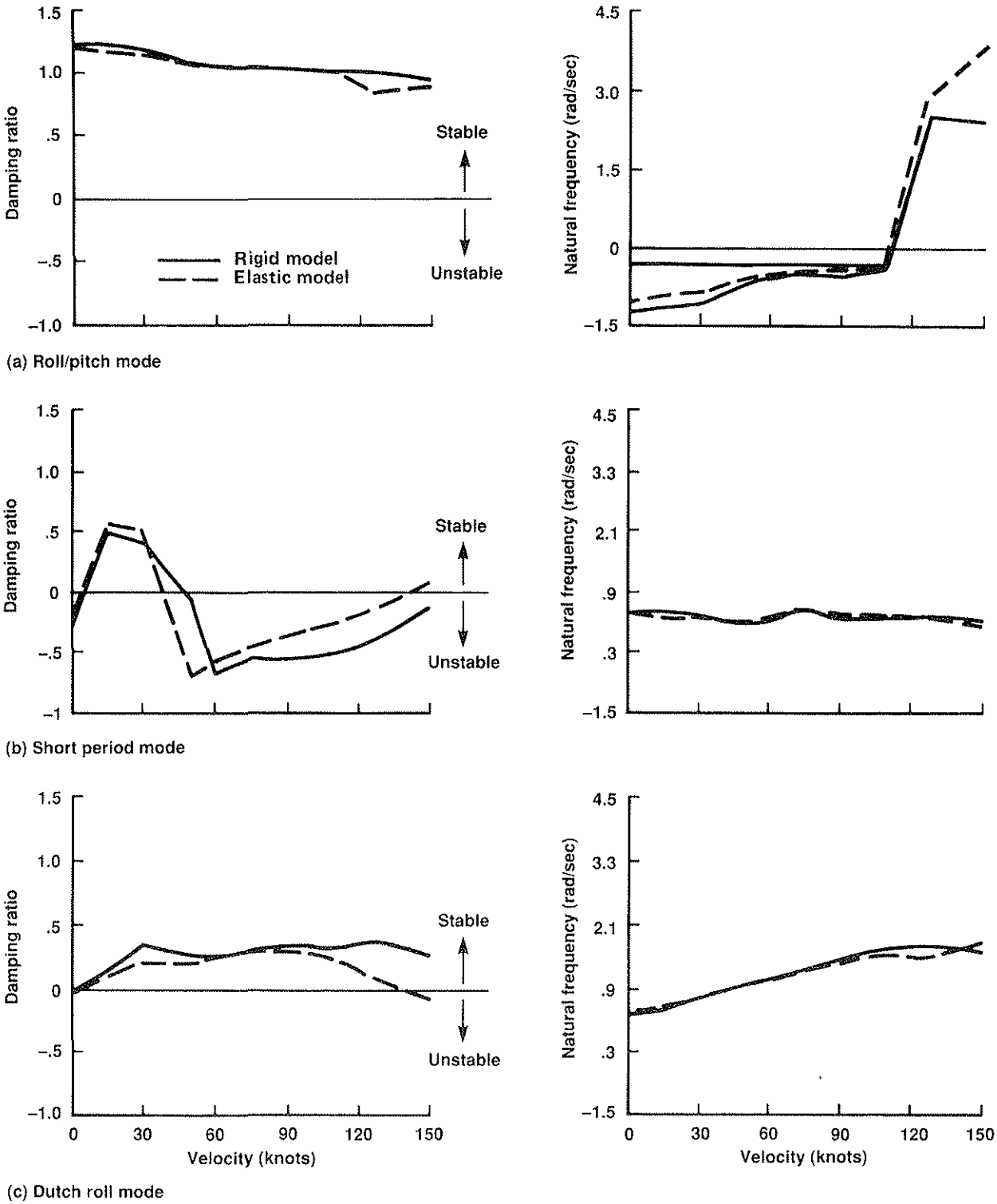

Figure 5. Damping and natural frequency for the open-loop roll/pitch, short period, and dutch roll modes.

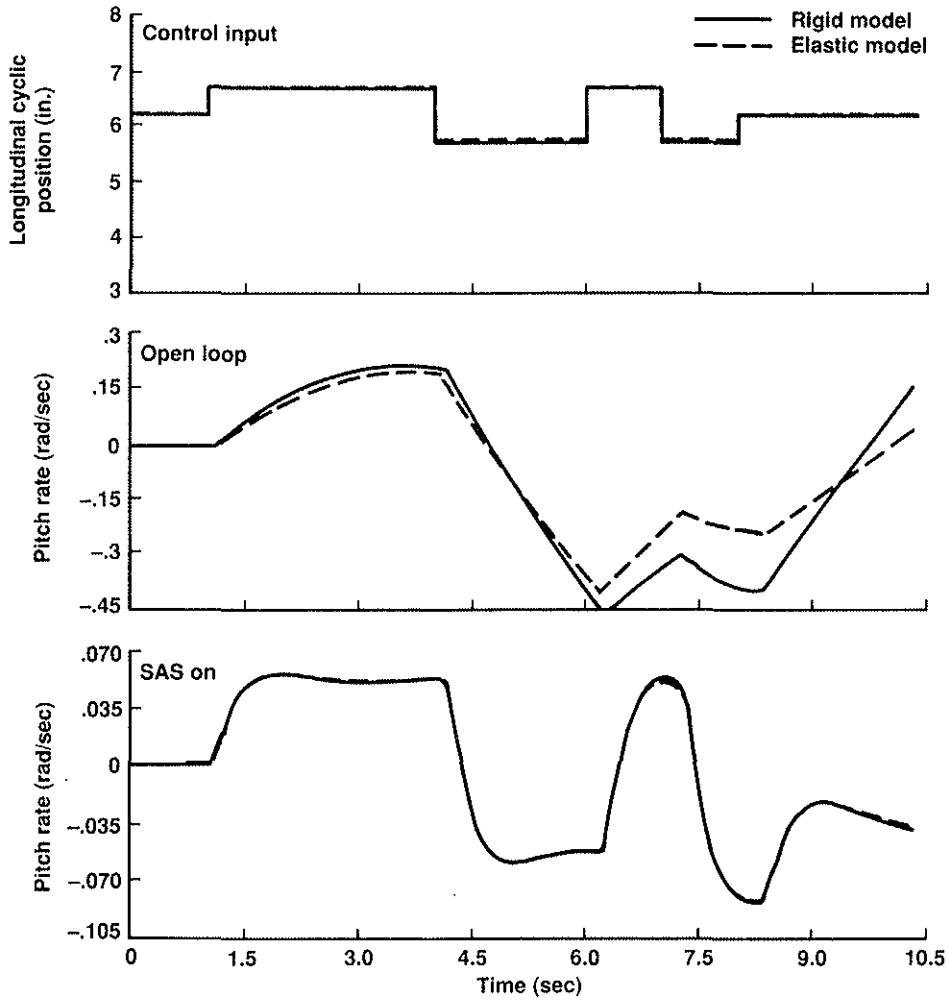

Figure 6. Dynamic comparison of rigid and elastic models at hover.

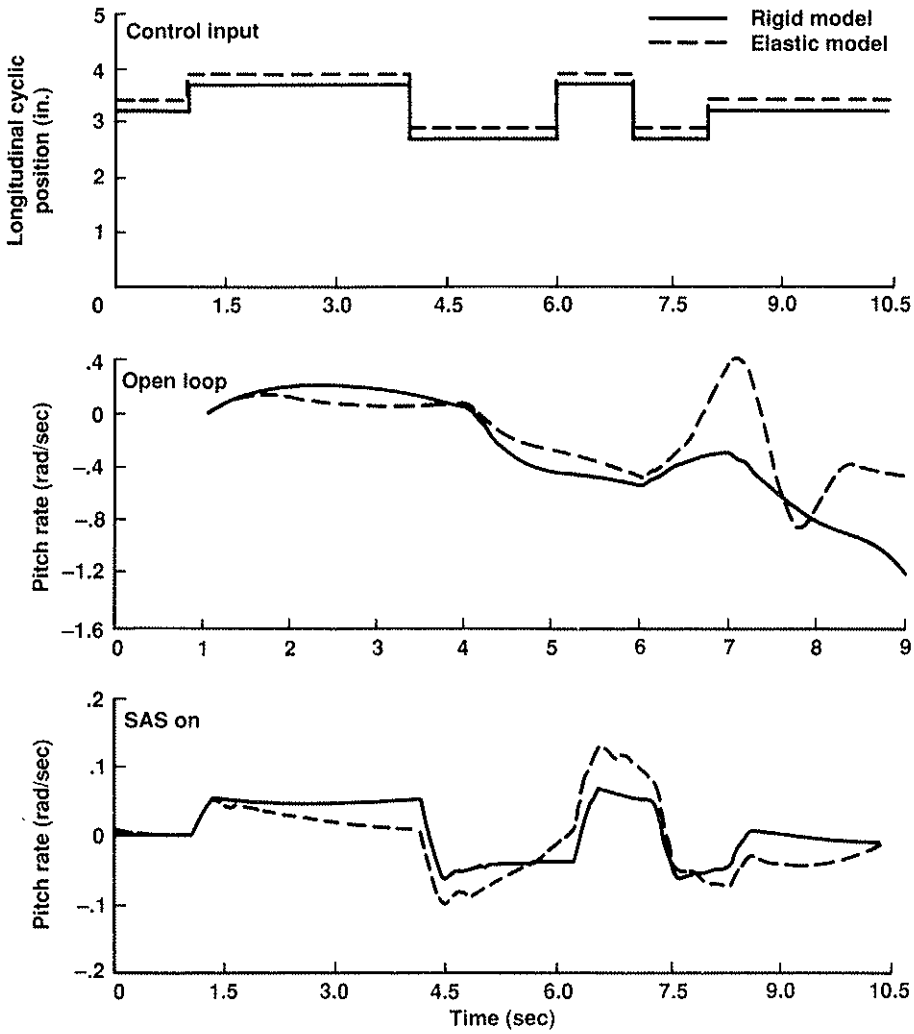

Figure 7. Dynamic comparison of rigid and elastic models at 150 knots.

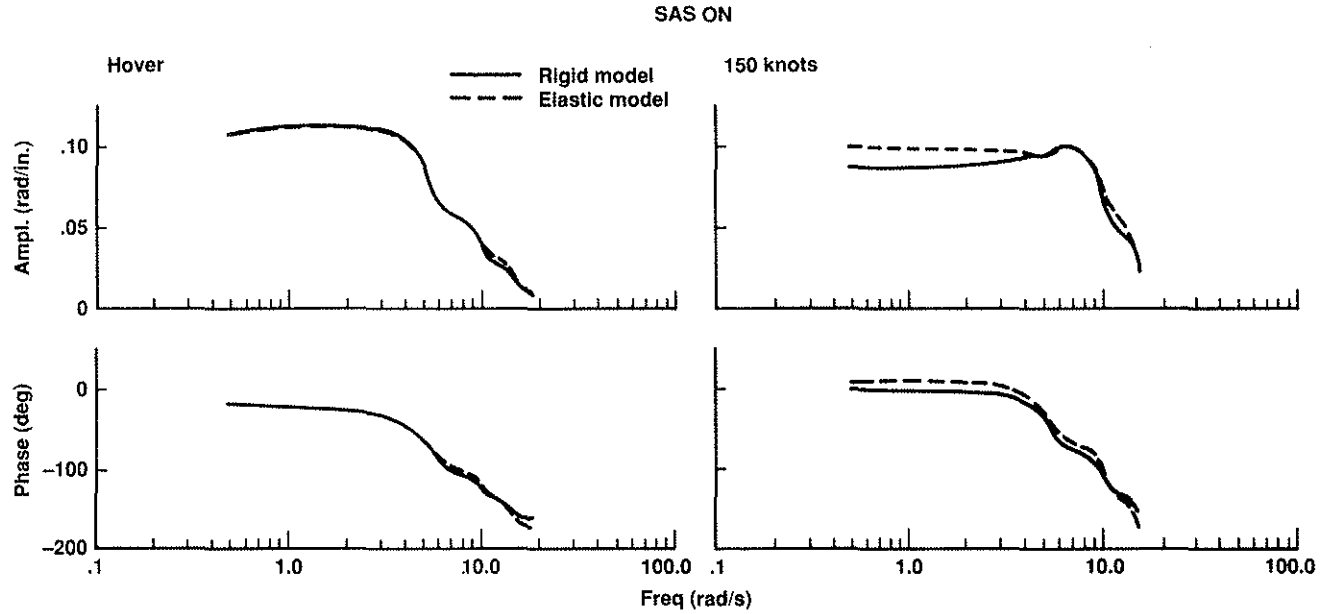

Figure 8. Comparison of rigid and elastic pitch-rate transfer function at hover and at 150 knots.

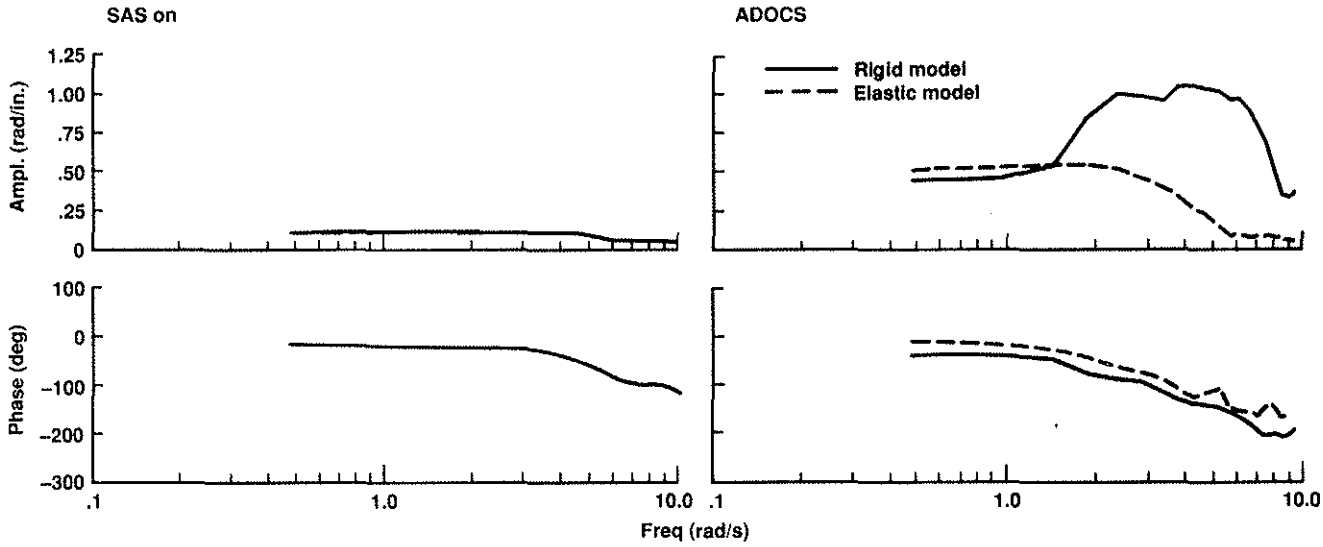

Figure 9. Comparison of rigid and elastic pitch-rate transfer function at hover for SAS and ADOCS controllers.

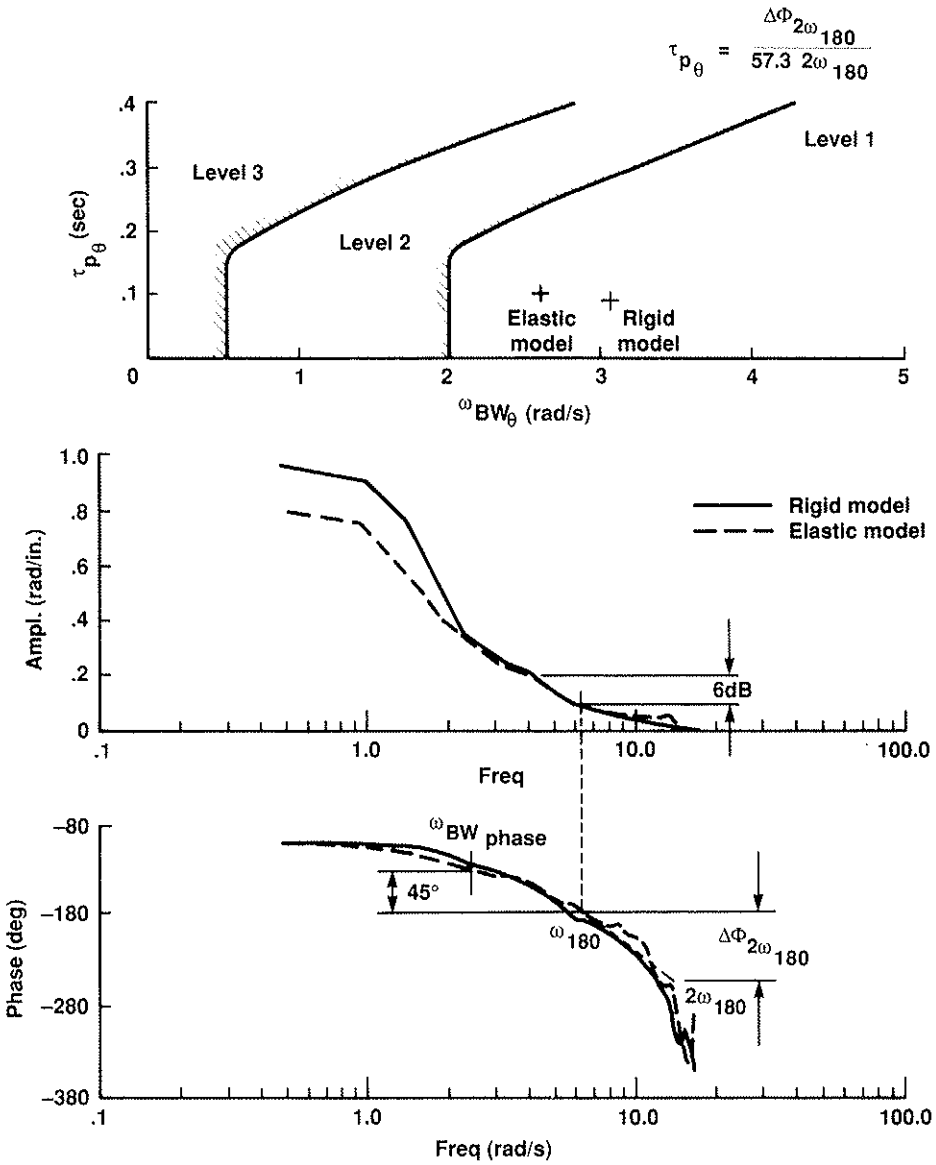

Figure 10. Short-term pitch response to control inputs using the ADOCS controller (80 knots) (air combat limits).

Maximum values for height response to collective controller

Level	$T_{\dot{h}_{eq}}$ (sec)	$\tau_{\dot{h}_{eq}}$ (sec)
1	5.0	0.20
2	∞	0.30

Actual values for height response to collective controller

Model	$T_{\dot{h}_{eq}}$ (sec)	$\tau_{\dot{h}_{eq}}$ (sec)
Rigid	1.7	0.17
Elastic	1.9	0.16

$$\dot{h}_{est}(t) = K\left[1 - e^{-\frac{1}{T_{\dot{h}_{eq}}}(t - \tau_{\dot{h}_{eq}})}\right]$$

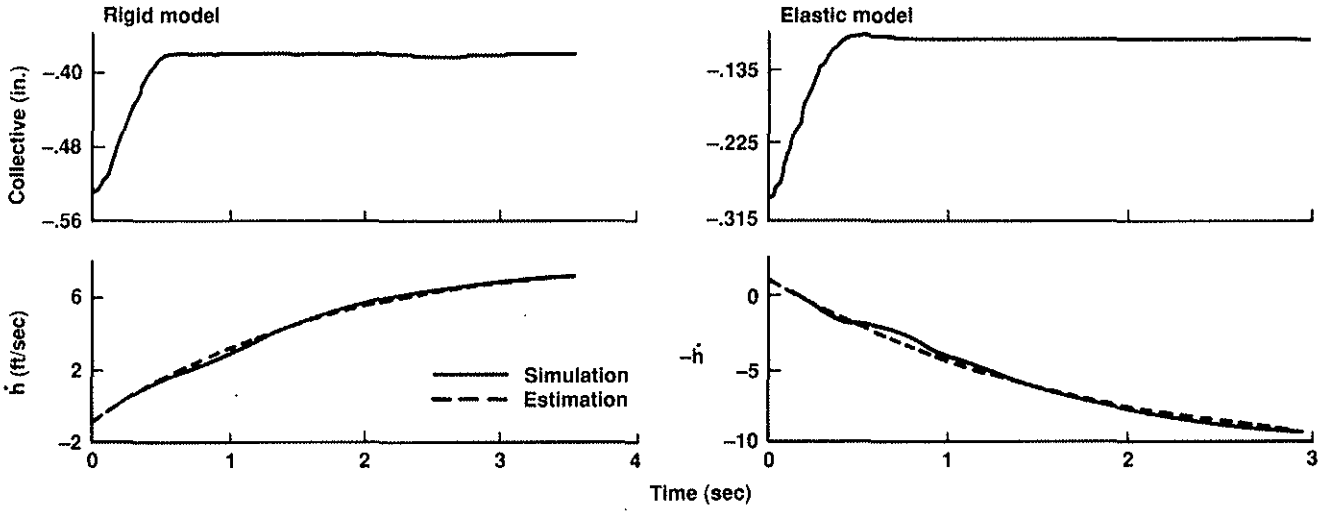

Figure 11. Vertical response to collective inputs using the ADOCS controller (hover).

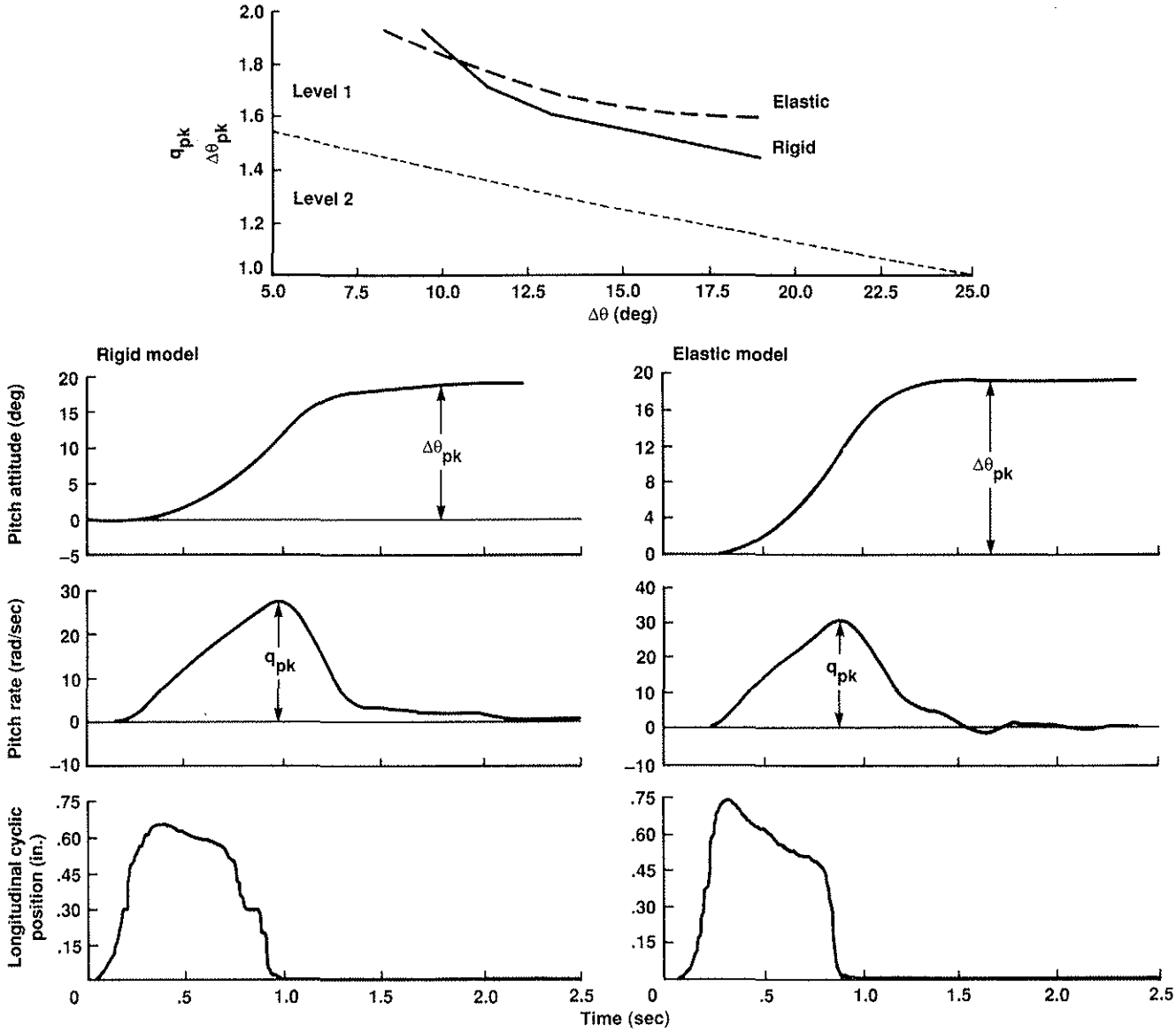

Figure 12. "Attitude quickness" comparisons for rigid and elastic models using the ADOCS controller (80 knots).